Skeletal Radiol (2000) 29:133–141

ARTICLE

Takashi Sakai
Nobuhiko Sugano
Takashi Nishii
Keiji Haraguchi
Takahiro Ochi
Kenji Ohzono

MR findings of necrotic lesions and the extralesional area of osteonecrosis of the femoral head

Received: 3 August 1999
Revision requested: 28 September 1999
Revision received: 11 November 1999
Accepted: 2 December 1999

T. Sakai, M.D. (✉),
N. Sugano, M.D., D.M.Sc.,
T. Nishii, M.D., D.M.Sc.,
K. Haraguchi, M.D.,
T. Ochi, M.D., D.M.Sc.,
K. Ohzono, M.D., D.M.Sc.
Department of Orthopedic Surgery,
Osaka University Medical School,
2-2 Yamadaoka, Suita, 565-0871, Osaka,
Japan

Abstract *Objective.* To investigate the MR findings of necrotic lesions and the extralesional area of osteonecrosis of the femoral head (ONFH) for each of the radiological stages.
Design and patients. Forty-nine hips in 29 patients (15 female, 14 male; mean age 38 years, range 17–59 years) were imaged using a 1.0-T superconducting magnet. T2-weighted spin echo pulse sequences (T2WI), spoiled gradient recalled echo pulse sequences (SPGR) and fat suppression SPGR (FS-SPGR), followed by Gd-DTPA enhanced fat suppression SPGR (Gd-FS-SPGR), were all obtained with the aid of a TORSO surface coil.
Results and conclusions. While a normal fat intensity area with a low-intensity band on SPGR (band pattern) was seen in 16 of 16 stage 1 (100%), nine of 11 stage 2 (82%), four of 17 stage 3 (24%), and none of five stage 4 hips, all hips showed peripheral rim enhancement on Gd-FS-SPGR (100%). This enhancement band on Gd-FS-SPGR corresponded to histological findings of necrotic trabecular bone, repaired marrow, and fibrous reparative tissue. Bone marrow edema was also clearly demonstrated as a diffuse, high-intensity area outside this enhancement band on Gd-FS-SPGR in two stage 2 (18%), 12 stage 3 (71%), and one stage 4 hip (20%). In cases at stage 2 or more advanced stages with homogeneous or inhomogeneous low intensity on nonenhanced MRI, the reparative process both inside and outside the necrotic lesion, including bone marrow edema, was detected clearly on contrast-enhanced MRI.

Key words Osteonecrosis of the femoral head (ONFH) · Magnetic resonance imaging (MRI) · Gd-DTPA · Fat suppression · Radiological stage · Bone marrow edema

Introduction

Magnetic resonance imaging (MRI) is highly sensitive for the diagnosis of osteonecrosis of the femoral head (ONFH) [1, 2]. A normal fat intensity area with a surrounding low-intensity band on T1-weighted images (T1WI) (band pattern) [3–6] and a double line sign on T2-weighted images (T2WI) [7] are seen in many patients with stage 1 (preradiological stage) and stage 2 disease (radiologically noncollapsed stage) of the ARCO (Association Research Circulation Osseous) international classification of ONFH (Table 1) [8]. These findings are defined as the boundary of necrotic lesions [7]. However, determining the location and extent of necrotic lesions has remained difficult in patients with stage 3 (radiological collapsed stage) and stage 4 disease because both necrotic lesions and reparative areas are shown as either homogeneous or inhomogeneous low-intensity areas on T1WI [7, 9–12], although T2WI can sometimes differentiate between necrotic tissue as fat-like or low-intensity, and reactional tissue as intermediate-intensity areas.

Table 1 ARCO (Association of Research Circulation Osseous) international staging system of osteonecrosis of the femoral head

Stage 0:	All diagnostic studies normal; diagnosis by histology only
Stage 1:	Plain radiographs, computed tomography normal; magnetic resonance imaging scintigraphy+; biopsy+; extent of involvement A, B, or C
Stage 2:	Radiographs+ but no collapse; extent of involvement A, B, or C
Stage 3:	Early flattening of dome, crescent sign; computed tomography or tomographs may be needed; extent of involvement A, B, or C; further characterization by amount of depression (in millimeters)
Stage 4:	Flattening of femoral head with joint space narrowing; possible other signs of early osteoarthritis

MRI is also useful for determining the pathophysiology of ONFH in both advanced [7, 9–13] and early stages [14]. Because MRI signal intensity is affected by tissue, which is composed of water and fat, there is a good correlation between MRI and the histological findings. However, previous histological studies have focused mainly on the necrotic area, which is surrounded by a low-intensity band on T1WI or a double line sign on T2WI, while little attention has been paid to the extralesional areas.

This study was undertaken to determine the MR findings of the necrotic lesions and the extralesional area of ONFH, including contrast-enhanced MR findings for each of the radiological stages.

Patients and methods

Between February 1998 and October 1998, 49 hips in 29 patients with ONFH, who had pain around the hip, were imaged (15 women, 14 men; mean age 38 years, range 17–59 years) using a 1.0-T superconducting magnet. Twenty-two patients had been treated with corticosteroid therapy (steroid-related necrosis), five patients had a history of alcohol abuse (alcohol-related necrosis), and two patients had no identifiable etiological factor for osteonecrosis (idiopathic necrosis). The underlying diseases for steroid-related necrosis were systemic lupus erythematosus in 11 patients, and idiopathic thrombocytopenic purpura, nephrotic syndrome, Harada's disease, pemphigus, idiopathic deafness, dermatomyositis, cerebral aneurysm, and glioblastoma in one each. Two patients underwent bone marrow transplantation, and one, renal transplantation. Sixteen hips in 13 patients underwent surgical treatment: 12 hips in nine patients underwent total hip arthroplasty, two hips in two patients underwent surface replacement, and two hips in two patients underwent anterior rotational osteotomy of the femoral head. Total hip arthroplasty was performed within a mean of 15.6 days (range 2–39 days) after the MRI examination.

Radiological stage

All patients were examined with anteroposterior and lateral radiographs of the femoral heads. The lateral view radiograph was obtained with the patient positioned supine with the hip at 90° flexion, 45° abduction, and neutral rotation. If the patient did not possess an adequate range of motion, the body of the patient was rotated so that the film was positioned parallel to the femoral neck [15]. The radiological stage was assessed according to the ARCO international classification of ONFH [8].

MR imaging

Cross-sectional images in the coronal plane were obtained with a TORSO surface coil. All sequences used a matrix size of 256×256, 1.5-mm slice thickness without an interslice gap, a field of view of 320 mm and one acquisition. Initially, T2-weighted spin echo pulse sequences (T2WI, repetition time (TR)/echo time (TE)=3600/105 ms), spoiled gradient recalled echo pulse sequences (SPGR, TR/TE=14/2.3 ms) and fat suppression SPGR (FS-SPGR) were obtained. The fat saturation pulse amplitude and frequency were optimized during the pre-imaging procedure (fat sat pulse). After these first three sequences had been obtained, a bolus of 0.1 mmol of Gd-DTPA (Magnevist, Schering, Berlin, Germany) per kilogram body weight was injected into the cubital vein. Within 5 min after the Gd-DTPA injection, Gd-DTPA enhanced fat suppression SPGR (Gd-FS-SPGR) was also obtained.

The MR findings of the necrotic area, the boundary of the necrotic lesion, and the extralesional area of the femoral head were assessed. The occurrence of reactive changes was defined as a low-intensity area on SPGR, intermediate- or low-intensity area on T2WI, and an enhanced area on Gd-FS-SPGR. Bone marrow edema was defined comparing post-Gd with pre-Gd enhancement images, as a diffuse low-intensity area on SPGR, a diffuse high-intensity area on T2WI, a diffuse intermediate- or high-intensity area on FS-SPGR and a diffuse enhanced area on Gd-FS-SPGR. A low-intensity band on SPGR separating the normal fat intensity area (band pattern) or double line sign on T2WI is considered to be a typical representation of ONFH [3–6]. We also checked how frequently this band pattern and double line sign could be seen on the central coronal image of the femoral head for each of the radiological stages. For the non-band-pattern hips, the boundary of the necrotic lesion was defined as a low-intensity band on SPGR or a peripheral rim enhancement band on Gd-FS-SPGR, which consisted of a continuous enhanced line around the necrotic lesion.

Histological study

The femoral heads of 12 hips in nine patients (10 stage 3 and two stage 4 hips) were resected at the time of total hip arthroplasty. They were fixed in neutrally buffered 10% formalin, decalcified, embedded in paraffin wax, sectioned to a thickness of 5 μm, and stained with hematoxylin and eosin. A histological diagnosis of ONFH was established when there was evidence of trabecular and marrow necrosis (necrotic zone) adjacent to viable bone and marrow (viable zone) with an intervening zone of repair (reparative zone) on the same section. The boundary of necrotic lesion was defined as an intervening zone of repair. The coronal section was compared with cross-sectional MR images in the coronal plane.

Statistical analysis

The chi-square test was used for statistical analysis, and a P value of less than 0.05 was considered significant.

Table 2 MR findings in the necrotic lesions and the extralesional area in stage 1 hips (preradiological stage, *n*=16) (*SPGR* spoiled gradient recalled echo pulse sequence (14/2.3), *T2WI* T2-weighted spin echo pulse sequence (3600/105), *FS-SPGR* fat supression SPGR, *Gd-FS-SPGR* Gd-DTPA enhanced fat suppression SPGR)

MR conditions	Band pattern on SPGR[a] (%) Double line sign on T2WI[b] (%)	No. of hips (case no.)	MRI signal intensity			
			Intralesional	Boundary	Extralesional (along the boundary)	Extralesional (within the femoral head)
SPGR	16 (100)	16[a] (1–16)	High/intermediate (normal fat intensity)	Low-intensity band	High	High
T2WI	14 (88)	14[b] (1–14)	High (normal fat intensity)	Double line/low-intensity band	High	High
		2 (15,16)	Low/high inhomogeneous	Low-intensity band	High	High
FS-SPGR		16 (1–16)	Low	Intermediate-intensity band	Low	Low
Gd-FS-SPGR		16 (1–16)	Low	Peripheral rim enhancement band	Low	Low

[a] Band pattern on SPGR consisted of normal fat intensity with a low-intensity band
[b] Double line sign on T2WI consisted of normal fat intensity with double line or a low-intensity band

Table 3 MR findings in the necrotic lesions and the extralesional area in stage 2 hips (radiological noncollapsed stage, *n*=11) (*SPGR* spoiled gradient recalled echo pulse sequence (14/2.3), *T2WI* T2-weighted spin echo pulse sequence (3600/105), *FS-SPGR* fat supression SPGR, *Gd-FS-SPGR* Gd-DTPA enhanced fat suppression SPGR)

MR conditions	Band pattern on SPGR[a] (%) Double line sign on T2WI[b] (%)	No. of hips (case no.)	MRI signal intensity			
			Intralesional	Boundary	Extralesional (along the boundary)	Extralesional (within the femoral head)
SPGR	9 (82)	8[a] (1–8)	High/intermediate (normal fat intensity)	Low-intensity band	High	High
		1[a] (9)	High/intermediate (normal fat intensity)	Low-intensity band	Low[c]	High
		1 (10)	Low	Low-intensity band	High	High
		1 (11)	Low	Low-intensity band	Low[c]	High
T2WI	8 (73)	8[b] (1–8)	High (normal fat intensity)	Double line/low-intensity band	High	High
		1 (10)	Low/high inhomogeneous	Low-intensity band	High	High
		2 (9, 11)	Low/high inhomogeneous	No band	(High)	High
FS-SPGR		9 (1–8, 10)	Low	Intermediate-intensity band	Low	Low
		2 (9, 11)	Intermediate	Intermediate-intensity band	Intermediate[c]	Low
Gd-FS-SPGR		9 (1–8, 10)	Low	Peripheral rim enhancement band	Low	Low
		2 (9, 11)	Intermediate	Peripheral rim enhancement band	High[c]	Low

[a] Band pattern on SPGR consisted of normal fat intensity with a low-intensity band
[b] Double line sign on T2WI consisted of normal fat intensity with double line or a low-intensity band
[c] Diagnosed as bone marrow edema

Results

Radiological stage and typical MR representations

Radiological stage and MR findings are shown in Tables 2–5. There were 16 hips in radiological stage 1, 11 hips in stage 2, 17 hips in stage 3, and five hips in stage 4. In one stage 4 hip, the femoral head had severely collapsed and the extent of the necrotic lesions could not be detected on the central coronal MR image. Therefore, this hip was excluded from the analysis. Two stage 2 hips collapsed and progressed to stage 3 within 6 months after the MR examination (Table 3, cases 9 and 11). Sixteen of 16 stage 1 (100%), nine of 11 stage 2 (82%), and four of 17 stage 3 (24%) hips showed normal fat intensity with a surrounding low-intensity band on SPGR (band pattern; Figs. 1A, 2A). Fourteen of 16 stage 1 (88%), eight of 11 stage 2 (73%), and two of 17 stage 3 hips (12%) showed normal fat intensity with a surrounding double line or low-intensity band on T2WI (double line sign, Figs. 1B, 2B). No stage 4 hips showed either the band pattern or the double line sign.

Frequency of reactive changes

A comparison of pre- with post-Gd enhancement images found that all hips showed peripheral rim enhancement of the boundary in the form of a reparative area on Gd-FS-SPGR (Figs. 1C,D, 2C,D). Intralesional reactive changes were observed near the boundary in six of 48 femoral head lesions. The presence of intralesional reactional changes was seen in none of the hips with stage 1 lesions, two hips (18%) with stage 2 lesions (Table 3, cases 9 and 11), one hip (6%) with stage 3 lesions (Table 4, case 5), and three hips (75%) with stage 4 lesions (Table 5, cases 1–3). In the extralesional area, reactive changes were observed in the form of bone marrow edema along the boundary in 15 of 48 femoral head lesions. Extralesional reactional changes were observed in two stage 2 hips (18%) (Table 3, cases 9 and 11), 12 stage 3 hips (71%) (Table 4, cases 1–4, 10–17), and one stage 4 hip (25%) (Table 5, case 4). The two stage 2 hips corresponded to the two collapsed stage 2 hips (Table 3, cases 9 and 11), in which bone marrow edema was seen outside the necrotic lesions (Fig. 3 left hip A–D, Fig. 4 left hip A–D). The frequency of extralesional reactive changes in stage 3 lesions was significantly higher than in other groups (chi-square test, P=0.0001).

Histopathological findings in reactional changes

Histological findings for 12 femoral heads are shown in Table 6. Histological examinations of the intralesional areas with high intensity on SPGR or T2WI showed tra-

Table 4 MR findings in the necrotic lesions and the extralesional area in stage 3 hips (radiological collapsed stage, n=17) (*SPGR* spoiled gradient recalled echo pulse sequence (14/2.3), *T2WI* T2-weighted spin echo pulse sequence (3600/105), *FS-SPGR* fat supression SPGR, *Gd-FS-SPGR* Gd-DTPA enhanced fat suppression SPGR)

MR conditions	Band pattern on SPGR[a] (%) Double line sign on T2WI[b] (%)	No. of hips (case no.)	MRI signal intensity: Intralesional	Boundary	Extralesional (along the boundary)	Extralesional (within the femoral head)
SPGR	4 (24%)	4[a] (1–4)	High/intermediate (normal fat intensity)	Low-intensity band	Low[c]	High
		5 (5–9)	Low or low/high inhomogeneous	Low-intensity band	High	High
		8 (10–17)	Low or low/high inhomogeneous	Low-intensity band	Low[c]	High
T2WI	2 (12%)	2 (1, 10)	High/intermediate (normal fat intensity)	Low-intensity band	High	High
		9 (2, 3, 5, 9, 11–15)	Low/high inhomogeneous	Double line/low-intensity band	High	High
		6 (4, 6–8, 16, 17)	Low/high inhomogeneous	No band	(High)	High
FS-SPGR		4 (6–9)	Low	Intermediate-intensity band	Low	Low
		12 (1–4, 10–17)	Low	Intermediate-intensity band	Intermediate[c]	Low
		1 (5)	Intermediate	Intermediate-intensity band	Low	Low
Gd-FS-SPGR		4 (6–9)	Low	Peripheral rim enhancement band	Low	Low
		12 (1–4, 10–17)	Low	Peripheral rim enhancement band	High[c]	Low
		1 (5)	Intermediate	Peripheral rim enhancement band	Low	Low

[a] Band pattern on SPGR consisted of normal fat intensity with a low-intensity band.
[b] Double line sign on T2WI consisted of normal fat intensity with double line or a low- intensity band
[c] Diagnosed as bone marrow edema

Table 5 MR findings in the necrotic lesions and the extralesional area in stage 4 hips (osteoarthritic stage, *n*=5) (*SPGR* spoiled gradient recalled echo pulse sequence (14/2.3), *T2WI* T2-weighted spin echo pulse sequence (3600/105), *FS-SPGR* fat supression SPGR, *Gd-FS-SPGR* Gd-DTPA enhanced fat suppression SPGR)

MR conditions	Band pattern on SPGR[a] (%) Double line sign on T2WI[b] (%)	No. of hips (case no.)	MRI signal intensity			
			Intralesional	Boundary	Extralesional (along the boundary)	Extralesional (within the femoral head)
SPGR	0 (0)	3 (1–3)	Low	Low-intensity band	High	High
		1 (4)	Low/high inhomogeneous	Low-intensity band	Low[c]	High
		1 (5)	High[d]	No band[d]	High[d]	High[d]
T2WI	0 (0)	3 (1–3)	Low/high inhomogeneous	Low-intensity band	High	High
		1 (4)	Low/high inhomogeneous	No band	High	High
		1 (5)	High[d]	No band[d]	High[d]	High[d]
FS-SPGR		3 (1–3)	Intermediate	Intermediate-intensity band	Low	Low
		1 (4)	Low	intermediate-intensity band	Intermediate[a]	Low
		1 (5)	Low[d]	No band[d]	Low[d]	Low[d]
Gd-FS-SPGR		3 (1–3)	Intermediate	Peripheral rim enhancement band	Low	Low
		1 (4)	Low	Peripheral rim enhancement band	High[c]	Low
		1 (5)	Low[d]	No band[d]	Low[d]	Low[d]

[a] Band pattern on SPGR consisted of normal fat intensity with a low-intensity band
[b] Double line sign on T2WI consisted of normal fat intensity with double line or a low-intensity band
[c] Diagnosed as bone marrow edema
[d] The femoral head was severely collapsed and necrotic lesions could not be detected on MRI

Table 6 Comparison of the MR findings and the histological findings (*n*=12) (*SPGR* spoiled gradient recalled echo pulse sequence (14/2.3), *T2WI* T2-weighted spin echo pulse sequence (3600/105), *FS-SPGR* fat supression SPGR, *Gd-FS-SPGR* Gd-DTPA enhanced fat suppression SPGR)

MR conditions	No. of hips	SPGR	T2WI	FS-SPGR	Gd-FS-SPGR	Histological findings
Intralesional	1	High (normal fat intensity)	High (normal fat intensity)	Low	Low	Trabecular microfracture, necrotic trabecular bone
	1	High (normal fat intensity)	Inhomogeneous low	Low	Low	Small eosinophilic debris, trabecular microfracture, necrotic trabecular bone
	1	Inhomogeneous low	High (normal fat intensity)	Low	Low	Small eosinophilic debris, trabecular microfracture, necrotic trabecular bone
	5	Diffuse low/ inhomogeneous low	Inhomogeneous low	Low	Low	Many eosinophilic debris, trabecular microfracture, necrotic trabecular bone
	4	diffuse low/ inhomogeneous low	inhomogeneous low	Intermediate	Intermediate	Eosinophilic debris, trabecular microfracture, necrotic trabecular bone with viable fibrous mesenchymal tissue
Boundary	8	Low-intensity band	Low-intensity band	Intermediate-intensity band	Peripheral rim enhancement band	Necrotic trabecular bone, repaired marrow with viable fibrous mesenchymal tissue
	4	Low-intensity band	No band	Intermediate-intensity band	Peripheral rim enhancement band	Necrotic trabecular bone, repaired marrow with viable fibrous mesenchymal tissue
Extralesional (along the boundary)	8	Low	High	Intermediate	High	Dilated vessels, interstitial edema
	4	High	High	Low	Low	Normal marrow
Extralesional (within the femoral head)	12	High	High	Low	Low	Normal marrow

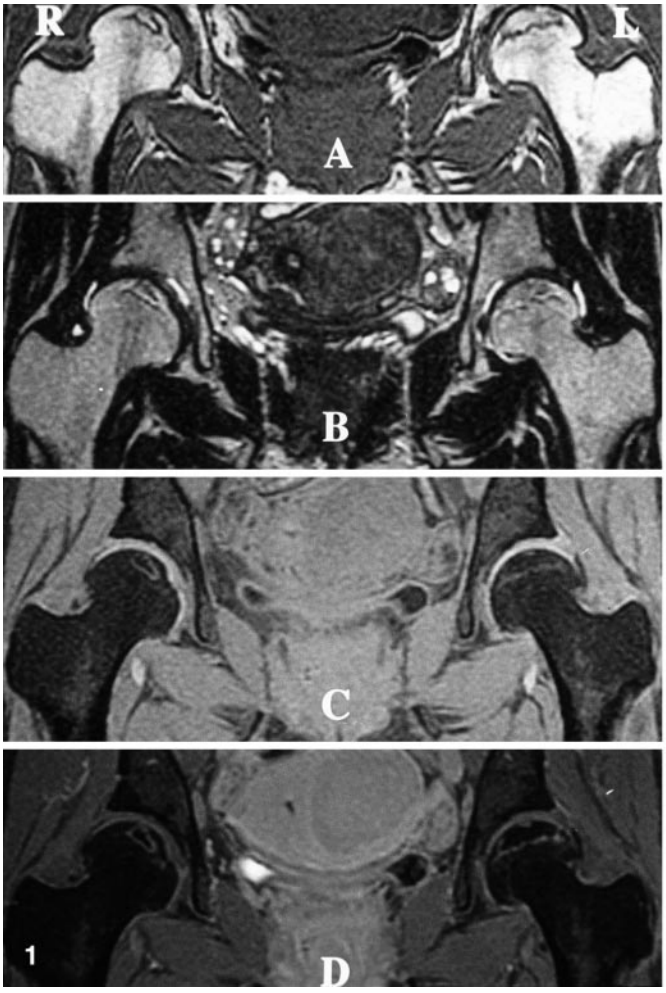

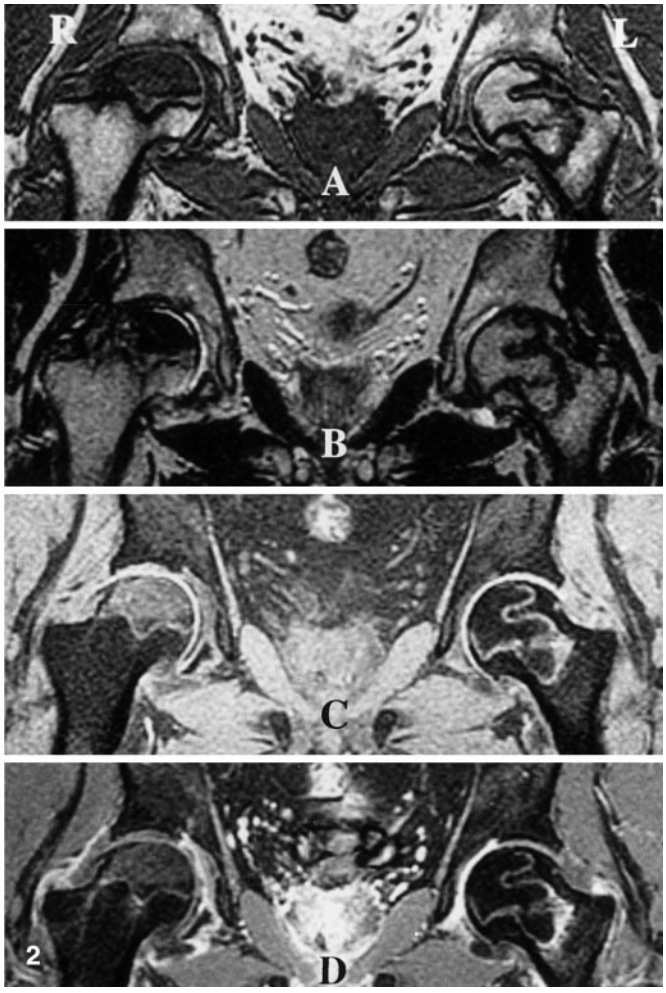

Fig. 1 Coronal MR images of bilateral hips of steroid-related stage 1 osteonecrosis of the femoral head (ONFH) in a 34-year-old woman: **A** SPGR (14/2.3), **B** T2WI (3600/105), **C** FS-SPGR, **D** Gd-FS-SPGR. The band pattern. Note the boundary was demonstrated as a low-intensity band on SPGR, a double line on T2WI, an intermediate-intensity band on FS-SPGR, and peripheral rim enhancement on Gd-FS-SPGR. The necrotic area was demonstrated as a normal fat intensity area on SPGR and T2WI, and a low-intensity area on FS-SPGR and Gd-FS-SPGR

Fig. 2 Coronal MR images of the right hip of steroid-related stage 3 ONFH and the left hip of stage 2 ONFH in a 47-year-old man: **A** SPGR (14/2.3), **B** T2WI (3600/105), **C** FS-SPGR, **D** Gd-FS-SPGR. Note the boundary was demonstrated as a low-intensity band on SPGR and T2WI, an intermediate-intensity band on FS-SPGR, and peripheral rim enhancement on Gd-FS-SPGR. The necrotic area of the right hip was demonstrated as low intensity on SPGR, inhomogeneous intensity on T2WI, and intermediate intensity on FS-SPGR and Gd-FS-SPGR. The necrotic area of the left hip was demonstrated as high intensity on SPGR and T2WI, and low intensity on FS-SPGR and Gd-FS-SPGR

becular microfractures and little marrow necrosis (three hips). Intralesional areas with low intensity on SPGR and T2WI showed much amorphous eosinophilic debris and many trabecular microfractures underneath the cartilage (five hips, Fig. 4E). Intralesional areas with intermediate intensity on Gd-FS-SPGR showed marrow necrosis and trabecular bone necrosis with viable fibrous mesenchymal tissue invading from the boundary (four hips). At the boundary of the lesions, necrotic trabecular bone with appositional bone formation was seen as well as fibrous reparative tissue filling the intertrabecular spaces (12 hips, Fig. 4F). Extralesional areas with bone marrow edema on Gd-FS-SPGR showed dilated vessels and interstitial edema, where the exudate of amorphous material was seen in the space between the adipocytes (eight hips; Fig. 4G). Extralesional areas with normal MR findings showed normal marrow tissue (area along the boundary in four hips and a more distal area within the femoral head in 12 hips).

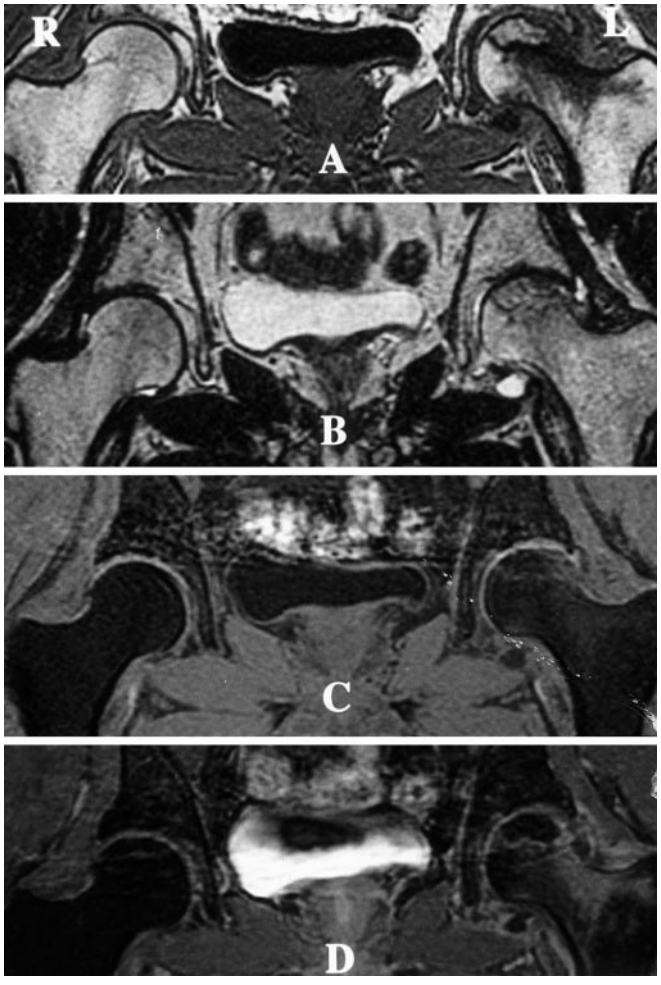

Fig. 3 Coronal MR images of the left hip of idiopathic stage 3 ONFH in a 48-year-old man: **A** SPGR (14/2.3), **B** T2WI (3600/105), **C** FS-SPGR, **D** Gd-FS-SPGR. The right hip was normal. Note Gd-FS-SPGR showed peripheral rim enhancement with a diffuse enhanced area outside the enhancement band extending to the femoral neck. This enhanced zone outside the peripheral rim enhanced band was diagnosed as bone marrow edema

Discussion

The band pattern on SPGR was detected in 29 (59%), while the double line sign on T2WI was detected in 24 of 49 (49%) hips. The pattern was detected at different stages depending on the extent of fat cell death. Although the fat cells may be dead, they still show high signal intensity unless they become necrotic, and necrosis occurs in the more extensive lesions. However, two stage 2 (18%), 13 stage 3 (76%), and four stage 4 hips (80%) showed either homogeneous or inhomogeneous low intensity on the central coronal nonenhanced images, which made it difficult to determine the extent and location of the necrotic lesions.

Reactive changes at each stage could be detected on FS-SPGR, and were confirmed more reliably by comparing pre- and post-Gd enhancement images. At the boundary of the necrotic lesions, reactive changes in all hips were detected on Gd-FS-SPGR in the form of a peripheral rim enhancement band in all hips. A comparison with the coronal sections of the femoral head showed that the peripheral rim enhancement band corresponded to necrotic trabecular bone with appositional bone formation, repaired marrow, and viable fibrous mesenchymal tissue, as also seen in the results of contrast-enhanced MRI [13, 14, 16–18]. Vande Berg et al. [13] compared contrast-enhanced MR findings with histological findings of ONFH in the advanced stage and reported that the enhanced area corresponded to viable fibrous mesenchymal tissue with marked sclerosis or with interstitial edema. Hauzeur et al. [14] compared contrast-enhanced MR findings with histological findings in 24 core biopsies and found Gd-DTPA-enhanced T1WI useful for ascertaining the presence of fibrosis associated with a thicker trabecular bone.

Intralesional reactive changes, seen as intermediate-intensity areas on Gd-FS-SPGR, were detected along the boundary mainly in stage 4 hips. They showed marrow necrosis and trabecular bone necrosis with viable fibrous mesenchymal tissue invading distally from the boundary. On the other hand, extralesional reactive changes were detected along the boundary most frequently in stage 3 hips in the form of dilated vessels and bone marrow edema. Vande Berg et al. [13] reported that interstitial edema was demonstrated as low intensity on T1WI, high intensity on T2WI, and as marked enhancement on contrast-enhanced images. Li and Hiette [16] also reported the presence of marrow areas with a diffuse edema pattern on Gd-FS-T1WI, which enhanced in the femoral head and neck extending into the femoral shaft. In a comparison with histological findings, the present study demonstrated bone marrow edema which was seen as a diffuse high-intensity zone in the extralesional area on Gd-FS-SPGR. The area of the edema did not involve the whole femoral head and all the edema was detected outside the boundary. The exact nature of bone marrow edema remains unknown; however, Kubo et al. [3] suggested in their study of renal allograft recipients with ONFH that bone marrow edema may be an inflammatory change in the reparative process after collapse of the femoral head, because it was detected most frequently in stage 3 hips and because two stage 2 hips with bone marrow edema collapsed and progressed to stage 3 within 6 months after the MR examination. Even if a hip had not radiologically collapsed (stage 2), detection of bone marrow edema on MRI may indicate that the femoral head has begun to collapse at the microscopic level. However, the present study could not confirm this because the numbers comparing MR findings directly with histological findings for all the collapsed hips were small.

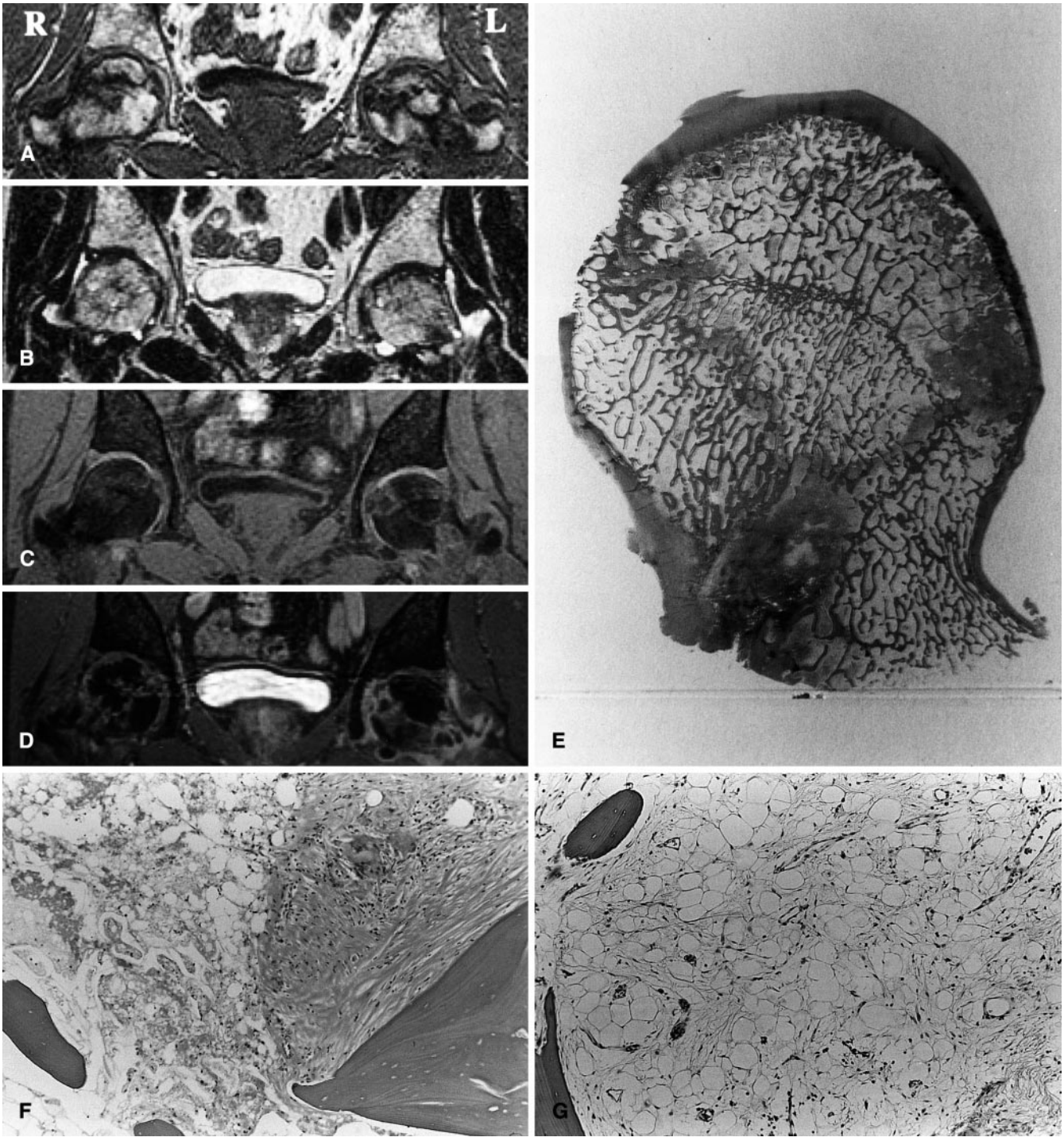

Fig. 4 Coronal MR images of the left hip of alcohol-related stage 3 ONFH in a 54-year-old man and a coronal section of the femoral head: **A** SPGR (14/2.3), **B** T2WI (3600/105), **C** FS-SPGR, **D** Gd-FS-SPGR, **E** gross section, **F** the boundary of the necrotic lesion (hematoxylin and eosin staining, ×40), **G** bone marrow edema outside the necrotic lesion (×40). The right hip also showed stage 3 ONFH. Note the amorphous eosinophilic debris and trabecular bone necrosis beneath the cartilage (**E**). At the boundary of the lesion, necrotic bone and eosinophilic debris (*left* in **F**) and necrotic bone with fibrous reparative tissue (*right* in **F**) are seen. An exudate of amorphous material is seen in the space between the adipocytes (bone marrow edema) (**G**). The peripheral rim enhancement band on Gd-FS-SPGR (**D**) corresponded with necrotic trabecular bone, repaired marrow, and the fibrous reparative tissue

Although the STIR (short TI inversion recovery) sequence has been employed to evaluate osteonecrosis [19], we could not use STIR for fat suppression because only a fat sat pulse could be used due to machine limitations. Clinically, STIR may be more useful when used with MRI apparatus with a low magnetic field or without equality of the magnetic field. However, the fat sat pulse for fat suppression has been widely used and the MRI apparatus used in the present study had sufficient equality of high magnetic field to assess bone marrow lesions.

In conclusion, the necrotic lesions of stage 1 ONFH are demonstrated clearly as a band pattern on SPGR. However, 18% of stage 2, 76% of stage 3, and 80% of stage 4 cases showed either homogeneous or inhomogeneous low intensity on nonenhanced images, which made determining the extent and location of the necrotic lesions difficult. In such cases, reactive changes could be demonstrated clearly on Gd-FS-SPGR. Intralesional reactive changes were detected along the boundary mainly in stage 4 hips, and the peripheral rim enhancement band was identified at the boundary in all cases. This band indicated marrow necrosis and trabecular bone necrosis with viable fibrous mesenchymal tissue. Extralesional reactive changes with diffuse enhancement were detected along the boundary most frequently in stage 3 hips in the form of dilated vessels and bone marrow edema, which may represent an inflammatory change in the reactive process after collapse of the femoral head in patients with ONFH.

References

1. Mitchell DG, Steinberg ME, Dalinka MK, Rao VM, Fallon M, Kressel HY. Magnetic resonance imaging of the ischemic hip: alterations within the osteonecrotic, viable, and reactive zones. Clin Orthop 1989; 244:60–77.
2. Hauzeur JP, Pasteels JL, Schoutens A, et al. The diagnostic value of magnetic resonance imaging in non-traumatic osteonecrosis of the femoral head. J Bone Joint Surg Am 1989; 71:641–649.
3. Kubo T, Yamazoe S, Sugano N, et al. Initial MRI findings of non-traumatic osteonecrosis of the femoral head in renal allograft recipients. Magn Reson Imaging 1997; 15:1017–1023.
4. Sugano N, Kubo T, Takaoka K, et al. Diagnostic criteria for non-traumatic osteonecrosis of the femoral head: a multicentre study. J Bone Joint Surg Br 1999; 81:590–595.
5. Sugano N, Ohzono K, Masuhara K, Takaoka K, Ono K. Prognostication of osteonecrosis of the femoral head in patients with systemic lupus erythematosus by magnetic resonance imaging. Clin Orthop 1994; 305:190–199.
6. Totty WG, Murphy WA, Ganz WI, Kumar B, Daum WJ, Siegel BA. Magnetic resonance imaging of the normal and ischemic femoral head. AJR 1984; 143:1273–1280.
7. Mitchell DG, Joseph PM, Fallon M, et al. Chemical-shift MR imaging of the femoral head: an in vitro study of normal hips and hips with avascular necrosis. AJR 1987; 148:1159–1164.
8. Stulberg BN. Editorial comment. Clin Orthop 1997; 334:2–5.
9. Bassett LW, Mirra JM, Cracchiolo A, Gold RH. Ischemic necrosis of the femoral head: correlation of magnetic resonance imaging and histologic sections. Clin Orthop 1987; 223:181–187.
10. Jergesen HE, Lang P, Moseley M, Genant HK. Histologic correlation in magnetic resonance imaging of femoral head osteonecrosis. Clin Orthop 1990; 253:150–163.
11. Lang P, Jergesen HE, Moseley ME, Block JE, Chafetz NI, Genant HK. Avascular necrosis of the femoral head: high-field-strength MR imaging with histologic correlation. Radiology 1988; 169:517–524.
12. Takatori Y, Kamogawa M, Kokubo T, et al. Magnetic resonance imaging and histopathology in femoral head necrosis. Acta Orthop Scand 1987; 58:499–503.
13. Vande Berg B, Malghem J, Labaisse MA, Noel H, Maldague B. Avascular necrosis of the hip: comparison of contrast-enhanced and nonenhanced MR imaging with histologic correlation. Radiology 1992; 182:445–450.
14. Hauzeur JP, Sintzoff S Jr, Appelboom T, Maertelaer VD, Bentin J, Pasteels JL. Relationship between magnetic resonance imaging and histologic findings by bone biopsy in nontraumatic osteonecrosis of the femoral head. J Rheumatol 1992; 19:385–392.
15. Sugano N, Takaoka K, Ohzono K, Matsui M, Masuhara K, Ono K. Prognostication of nontraumatic avascular necrosis of the femoral head: significance of location and size of the necrotic lesion. Clin Orthop 1994; 303:155–164.
16. Li KCP, Hiette P. Contrast-enhanced fat saturation magnetic resonance imaging for studying the pathophysiology of osteonecrosis of the hips. Skeletal Radiol 1992; 21:375–379.
17. Peiss J, Adam G, Casser R, Urhahn R, Gunther RW. Gadopentetate-dimeglumine-enhanced MR imaging of osteonecrosis and osteochondritis dissecans of the elbow: initial experience. Skeletal Radiol 1995; 24:17–20.
18. Uberoi R, Tai G, Hughes PM. Gadolinium-DTPA-enhanced MRI in the evaluation of osteonecrosis. Clin Radiol 1994; 49:645–648.
19. Nadel SN, Debatin JF, Richardson WJ, et al. Detection of acute avascular necrosis of the femoral head in dogs: dynamic contrast-enhanced MR imaging vs spin-echo and STIR sequences. AJR 1992; 159:1255–1261.